Düzce University
Journal of Science & Technology

Research Article

Visible Digital Image Watermarking Using Single Candidate Optimizer

Harun AKBULUT [a,*]

[a] *Department of Computer Engineering, Faculty of Engineering and Architecture, Nevsehir Haci Bektas Veli University, Nevşehir, TURKIYE*
** Corresponding author's e-mail address: harun.akbulut@nevsehir.edu.tr*
DOI: 10.29130/dubited.1532300

ABSTRACT

With the advent of internet technologies, accessing information has become remarkably facile, while concurrently precipitating copyright conundrums. This predicament can be ameliorated by embedding copyright information within digital images, a methodology termed digital image watermarking. Artificial intelligence optimization algorithms are extensively employed in myriad problem-solving scenarios, yielding efficacious outcomes. This study proposes a visible digital image watermarking method utilizing the Single Candidate Optimizer (SCO). Contrary to many prevalent metaheuristic optimization algorithms, SCO, introduced in 2024, is not population-based. The fitness function of SCO is designed to maximize the resemblance between the watermarked image and both the host and watermark images. Experiments were conducted on images commonly utilized in image processing, and the results were evaluated using eight quality metrics. Additionally, the obtained numerical results were juxtaposed with those from well-known and widely-used genetic algorithms, differential evolution algorithms, and artificial bee colony optimization algorithms. The findings demonstrate that SCO outperforms the others in visible digital image watermarking. Furthermore, due to its non-population-based nature, SCO is significantly faster compared to its counterparts.

Keywords: *Single candidate optimizer, Digital image watermarking, Metaheuristic optimization algorithms*

Tek Aday Optimizasyon Algoritması Kullanarak Görünür Dijital Resim Damgalama

ÖZ

İnternet teknolojilerinin gelişmesiyle birlikte bilgiye erişim çok kolay hale gelirken diğer taraftan telif hakkı problemini ortaya çıkarmıştır. Bu problem dijital resimlerin içerisine telif hakkı ile ilgili bilgi gömerek çözülebilmektedir. Bu yöntemlere dijital resim damgalama denir. Yapay zeka optimizasyon algoritmaları bir çok problem çözümünde kullanılmakta ve etkili sonuçlar vermektedir. Bu çalışmada Single candidate optimizer (SCO) kullanarak görünür dijital görüntü damgalama yöntemi önerilir. 2024 yılında önerilen SCO, bir çok yaygın meta-sezgisel optimizasyon algoritmasının aksine popülasyon tabanlı değildir. SCO'nun amaç fonksiyonu olarak damgalanmış görüntünün hem barındırıcı hem de damga görüntüsü ile benzerliğini maksimize eden fonksiyon kullanılır. Deneyler görüntü işlemede yaygın kullanılan görüntülere uygulanmış ve sekiz adet kalite metriği kullanılarak sonuçlar değerlendirilmiştir. Ayrıca elde edilen sayısal sonuçlar iyi bilinen ve yaygın kullanılan genetik algoritma, diferansiyel gelişim algoritması ve yapay arı kolonisi optimizasyon algoritmaları ile karşılaştırılmıştır. Elde edilen bulgular SCO'nun görünür dijital görüntü damgalama için diğerlerinden daha iyi sonuç verdiğini göstermiştir. Ayrıca SCO'nun popülasyon tabanlı olmadığı için diğerlerine göre çok daha hızlı sonuç verdiği görülmüştür.

Received: 12/08/2024, Revised: 07/10/2024, Accepted: 20/11/2024

Anahtar Kelimeler: *Tek aday optimizasyon algoritması, dijital resim damgalama, meta-sezgisel optimizasyon algoritmaları*

I. INTRODUCTION

With the rapid advancement of information technologies, digital images, films, audio, and multimedia applications have become inextricable constituents of our quotidian existence, concomitantly engendering copyright dilemmas due to facile access to digital data. In recent years, scholars have devised digital watermarking techniques to ameliorate the copyright conundrums associated with digital content. Digital watermarking can be delineated as a method for embedding copyright data within the structure of digital content without compromising its integrity. This technique is prevalently employed for safeguarding the copyright of digital images. The process of embedding data within digital images can be executed either at the pixel level or in the frequency domain via various transformation methods. Moreover, digital watermarking can be classified into visible and invisible categories, contingent upon whether the embedded data is perceptible or not. Visible digital watermarking is characterized by the amalgamation of the host image and the watermark, necessitating that the watermark not only encapsulates maximal information from the host image but also retains its clarity while exhibiting robustness against potential attacks [1].

Scholars have propounded an array of watermarking-based methodologies to address challenges such as security, perceptibility, capacity, intricacy, and resilience. These methodologies can be fundamentally categorized into two distinct classes: spatial domain and frequency domain. In the former, the watermarked image is generated through a series of operations performed on individual pixels or pixel groups. In contrast, the latter approach involves manipulating the frequencies obtained within the transformation domain to produce the watermarked image. While the first method is characterized by its low computational cost and considerable robustness, the latter entails a higher computational burden. Moreover, in the second method, any error introduced during the manipulation of the combination coefficients during watermarking can propagate across the entire image, potentially resulting in an artificial watermarked image [1-2].

Single-domain approaches often fail to achieve satisfactory performance, necessitating the integration of multiple digital watermarking techniques to enhance efficacy. Anand et al. [3] introduced a dual watermarking method to bolster the security of COVID-19 patients, embedding both a logo and patient information to reinforce the integrity and authenticity of CT images. Roy et al. [4] developed a DCT-SVD hybrid watermarking technique aimed at copyright protection, wherein the scrambled watermark is embedded within DCT coefficient blocks, demonstrating superior robustness and high imperceptibility in simulations. Abdulrahman et al. [5] devised a color image watermarking system utilizing a DCT-DWT hybrid to ensure copyright protection. Additionally, an efficient block-based color image watermarking method embeds the watermark logo into the principal component to mitigate the false positive problem.

Numerous meta-heuristic algorithms have been extensively utilized in the literature to ascertain the optimal value of the multiple embedding factors. Darwish et al. [6] proposed a GA-based approach to integrate both sequential and segmented watermarking, utilizing the GA to identify suitable locations within the cover image. The dual watermarks are embedded into the YCbCr color channel via the Walsh-Hadamard Transform (WHT), significantly enhancing watermarking capacity and rendering the technique impervious to image manipulation attacks. Mittal et al. [7] employed an exponential k-best GSA (eKGSA) to determine optimal thresholds for multi-level image segmentation. Wang et al. [8] implemented a hierarchical gravity search algorithm to mitigate premature convergence and enhance search capacity. Rawal et al. [9] devised a fast convergent GSA, accelerating convergence and exploitation through a sigmoidal function and exponential step size. Additionally, Mittal et al. [10] introduced an advanced GSA, known as Intelligent GSA (IGSA), to improve convergence precision.

Aslantaş et al. [11] proposed a novel robust image watermarking technique based on the Discrete Cosine Transform (DCT) utilizing the Genetic Algorithm (GA). The GA was employed to optimize the mid-band frequency coefficients, and the proposed method demonstrated commendable efficacy. Zhang et al. [12] presented a watermarking method based on Curvelet and Arnold transforms, employing GA for optimizing threshold values to enhance the resilience of the watermarked image. Jagadeesh, and associates [13] developed an improved image watermarking technique grounded in Singular Value Decomposition (SVD) using GA. The GA was utilized to optimize the quantization step size, and the proposed method was shown to be more secure and robust against attacks such as low-pass filtering, median filtering, image compression, and resizing.

As previously mentioned, artificial intelligence optimization algorithms are employed in image watermarking methods and in solving a multitude of problems [14-17], yielding effective results. In this study, a visible digital image watermarking method is proposed utilizing the SCO, a non-population-based approach, in contrast to other meta-heuristic optimization algorithms suggested in 2024. The contributions of this work to the literature can be delineated as follows:

- The implementation of SCO, a relatively novel technique for visible digital image watermarking.
- The objective quality assessment of the watermarked images is conducted using eight quality metrics that are prevalently employed in the literature.
- The evaluation of the watermarked images also incorporates subjective assessment.
- A comparative analysis is undertaken with widely recognized and utilized meta-heuristic optimization algorithms, namely, Genetic Algorithm (GA), Differential Evolution (DE), and Artificial Bee Colony (ABC).

II. OPTIMIZED DIGITAL IMAGE WATERMARKING

A. SINGLE CANDIDATE OPTIMIZER (SCO)

The Single Candidate Optimizer (SCO) [18], proposed by Shami et al. in 2024, eschews the population-based method of traditional metaheuristic optimization algorithms, opting instead for a solitary candidate approach. This method updates the position of a single candidate, resulting in markedly accelerated solutions compared to its population-based counterparts. SCO employs a biphasic strategy to balance exploration and exploitation. In the initial phase, candidate solution positions are updated using Equation 1.

$$x_j = \begin{Bmatrix} gbest_j + (w|gbest_j|)\ if\ r_1 < 0.5 \\ gbest_j - (w|gbest_j|)\ otherwise \end{Bmatrix} \quad (1)$$

Here, r_1 is a randomly generated value between [0, 1].
In the second phase, SCO explores the vicinity of the best position obtained in the first phase, thereby identifying superior positions via Equation 2.

$$x_j = \begin{Bmatrix} gbest_j + ((r_2 w(ub_j - lb_j))\ if\ r_2 < 0.5 \\ gbest_j - ((r_2 w(ub_j - lb_j))\ otherwise \end{Bmatrix} \quad (2)$$

Here, r_2 is randomly generated value between [0, 1]. ub_j and lb_j denote the upper and lower bounds, respectively. w is the parameter that provides the balance between exploration and exploitation. w is obtained using Equation 3.

$$w^t = exp^{-\left(\frac{bt}{T}\right)^b} \quad (3)$$

Here, b is a constant, t is the current iteration number, and T is the maximum iteration number.

A principal challenge in metaheuristic optimization algorithms is their propensity to become ensnared in local optimum. To mitigate this issue, SCO leverages Equation 4.

$$x_j = \begin{Bmatrix} gbest_j + ((r_3(ub_j - lb_j))\ if\ r_3 < 0.5 \\ gbest_j - ((r_3(ub_j - lb_j))\ otherwise \end{Bmatrix} \quad (4)$$

Here, r_3 is randomly generated value between [0, 1].

Occasionally, problem boundaries may be transgressed, necessitating the application of normalization via Equation 5.

$$x_j = \begin{Bmatrix} gbest_j\ if x_j > ub_j \\ gbest_j\ if x_j < lb_j \end{Bmatrix} \quad (5)$$

SCO initiates the problem-solving process by generating a random solution, then iteratively updates the candidate's positions to converge upon an optimal solution. The initial candidate solution generation in SCO is calculated using Equation 6.

$$x_j = lb_j + r_4(ub_j - lb_j) \quad (6)$$

Subsequently, position updates are performed throughout the iterations using Equations 1 and 2. The newly obtained position is evaluated using the fitness function, and if it surpasses the known best solution, it is updated as the new optimal position. This process persists until the maximum iteration count, T, is reached. The fundamental steps of SCO are delineated in Algorithm 1.

Algorithm 1 Pseudo Code of SCO

```
Set c=0, p=0 and define the values of a and m
Generate the initial candidate solution using Eq (6) and calculate  fitness f(gbest)
while t<T do
    if t<a then
        Update position Eq (1)
    else
        if p=0 then
            c=c+1
        end if
        if c=m then
            c=0
            Update position Eq(4)
        else
            Update position Eq(2)
        end if
    end if
Calculate fitness f(x)
if f(x) is better than f(gbest) then
   gbest=x
   f(gbest)=f(x)
   p=1
else
   p=0
end if
t=t+1
end while
return gbest
```

B. VISIBLE DIGITAL IMAGE WATERMARKING USING SINGLE CANDIDATE OPTIMIZER

In the proposed methodology, an initial candidate solution is stochastically generated by the SCO algorithm with the lower bound set to 0 and the upper bound set to 1, employing Equation (6). Subsequently, utilizing this amalgamation coefficient, the host and watermark images are integrated via Equation (7).

$$WI = w * H + (1 - w) * W \tag{7}$$

Here, WI denotes the watermarked image, while w represents the amalgamation coefficient engendered by the SCO algorithm. H signifies the host image, and W denotes the watermark image, respectively.

The watermarked image is thus procured using Equation (7). Thereafter, the fitness function value of the watermarked image is ascertained using Equation (8). Throughout each iteration, the amalgamation coefficient is iteratively refined employing Equation (1), (2), and (4) to ascertain the optimal amalgamation coefficient.

$$Fitness = C(H, WI) + C(EW, W) \tag{8}$$

Here, H represents host image, WI represents watermarked image, W represents watermark image, EW represents extrapolated watermark image, $C(H, WI)$ represents the correlation coefficient between the H and WI and, $C(EW, W)$ represents the correlation coefficient between the EW and W. $C(H, WI)$ is calculated using equation 9. The block diagram of the proposed methodology is delineated in Figure 1.

$$C(H, WI) = \frac{\sum_m \sum_n (H_{mn} - \bar{H})(WI_{mn} - \overline{WI})}{\sqrt{(\sum_m \sum_n (H_{mn} - \bar{H})^2)((WI_{mn} - \overline{WI})^2)}} \tag{8}$$

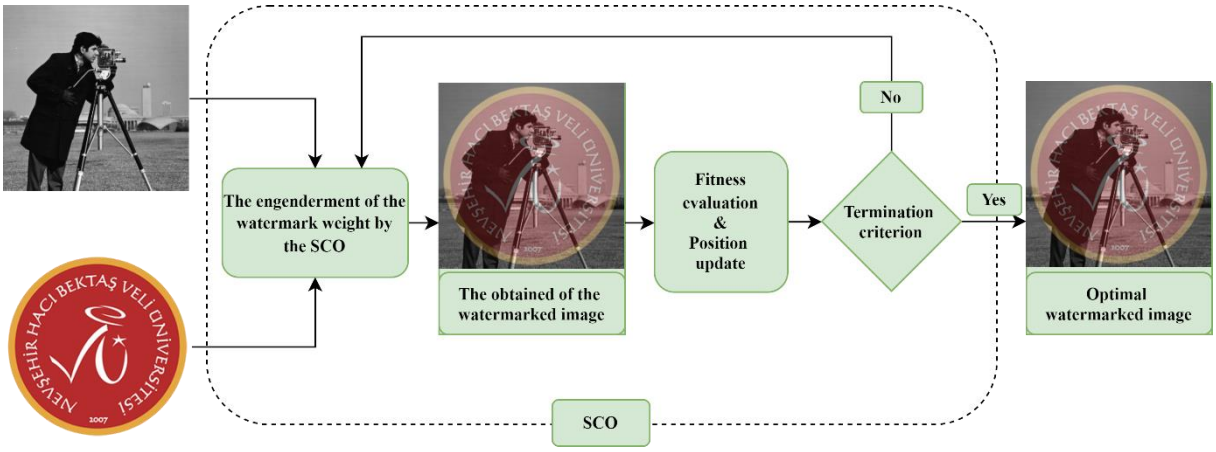

Figure 1. *A block diagram of visible image watermarking utilizing SVO*

C. THE OPTIMIZATION ALGORITHMS USED FOR COMPARISON

This section elucidates the metaheuristic optimization algorithms that are prevalently utilized and well-established in optimization problems, particularly in comparison with SCO. The metaheuristic optimization algorithms selected for comparison encompass the Genetic Algorithm (GA), which serves as a progenitor of population-based metaheuristic optimization algorithms inspired by evolutionary principles; the Differential Evolution Algorithm (DE),

which is a forerunner of deterministic population-based metaheuristic optimization algorithms; and the Artificial Bee Colony Optimization Algorithm, which is a pioneering representative of swarm intelligence-based metaheuristic optimization algorithms.

C. 1. Genetic Algorithm

The genetic algorithm (GA) [19], founded on natural selection and genetic principles, was developed by John Holland and his students in the 1960s. It is an efficacious tool for solving optimization problems. GA is a population-based algorithm that commences with a randomly generated initial population. The quality of solutions is assessed using a predefined objective function. Population size is a critical control parameter; an excessively large population increases computational cost, especially problematic in online applications, while a very small population diminishes the algorithm's ability to explore the search space and achieve global optimization.

GA employs genetic operators such as selection, crossover, and mutation. The selection operator favors high-quality individuals, enhancing their representation in subsequent generations, thereby progressing toward optimal solutions. The crossover operator combines two randomly chosen individuals from the solution pool to produce a new, high-quality individual, aiding in reaching the optimal solution and avoiding local optima. The mutation operator introduces random changes to a selected solution, fostering the discovery of previously unexplored high-quality individuals in the solution space.

C. 2. Differential Evolution Algorithms

The differential evolution algorithm (DE) [20] is a population-based, expeditious, and robust stochastic direct search optimization algorithm. DE can be employed to ascertain optimal solutions for nonlinear, non-differentiable, and multi-modal continuous space functions comprised of real parameters. Despite utilizing a heuristic algorithm structure, DE distinguishes itself through unique mechanisms for generating new solutions and its ‘greedy’ selection process. Similar to other evolutionary algorithms, DE employs operators such as initial population generation, crossover, mutation, and selection. The fundamental steps of DE include the formation of the initial population, evaluation of population individuals, mutation, crossover, and selection. These operators are sequentially and iteratively applied until a predetermined termination criterion, such as reaching the maximum number of iterations per generation, is satisfied

C. 3. Artificial Bee Colony Optimization Algorithms

The Artificial Bee Colony (ABC) [21] algorithm, developed by Karaboğa, is a recently advanced optimization algorithm based on swarm intelligence, modeling the intelligent foraging behaviors of honeybees for numerical problem optimization. In the ABC algorithm, food source regions represent potential solution values for the problem to be solved. The nectar amounts in food sources identified by scout bees correspond to the quality values of potential solutions. Worker bees are dispatched to the food sources detected by scout bees. These worker bees evaluate the quality of the food source they are working on and its neighboring sources, tending towards the source with better solution quality. When a worker bee returns to the hive with information about the current solution and the new position, it communicates this data to the onlooker bees through a dance. The higher the quality of the solution proposed by the worker bee, the greater the likelihood it will be selected by the onlooker bees. Once the food amount at

a source is depleted, indicated by reaching the threshold value set by the ABC algorithm's limit parameter, the worker bee becomes a scout bee and resumes exploration.

D. QUALITY METRICS

The appraisal of watermarked images' quality presents a challenge for researchers. Given the unique attributes of each watermarked image, a singular objective quality metric capable of evaluating all such images has yet to be devised. Consequently, it is imperative to assess the quality of a watermarked image using multiple metrics. In this study, eight widely recognized objective quality metrics from the literature have been employed. These quality metrics and their formulated representations are delineated in Table 1. The first column of Table 1 enumerates the name of the quality metric, followed by its abbreviation used in this paper, and the final column presents its formulated expression.

Table 1. *Quality metrics used for objective evaluation.*

Abbr	Name	Formulas
M_1	Variance [22]	$\mathrm{M}_1(F) = \frac{1}{mxn}\sum_{(i,j)}(F(i,j)-\mu)^2$
M_2	Entropy [23]	$\mathrm{M}_2(F) = -\sum_{i=0}^{L} h_f(i) log_2 h_f(i)$
M_3	Spatial frequency [24]	$M_3 = \sqrt{R^2 + C^2}$ $R = \sqrt{\frac{1}{mxn}\sum_i\sum_j [f(i,j)-f(i-1,j)]^2}$ $C = \sqrt{\frac{1}{mxn}\sum_i\sum_j [f(i,j)-f(i,j-1)]^2}$
M_4	Standard deviation [25]	$\mathrm{M}_4(F) = \sqrt{\sum_{i=0}^{L}(i-\bar{\imath})^2 log_2 h_f(i)}$
M_5	Edge based quality metric [26]	$\mathrm{M}_5(F) = \frac{\sum_{n=1}^{N}\sum_{m=1}^{M} Q^{AF}(n,m)w^A(n,m) + Q^{BF}(n,m)w^B(n,m)}{\sum_{n=1}^{N}\sum_{m=1}^{M}(w^A(n,m)+w^B(n,m))}$
M_6	Chen-Blum quality metric [27]	$\mathrm{M}_6(F) = Sm_A(x,y)Q_{AF}(x,y) + Sm_B(x,y)Q_{BF}(x,y)$ Here $Sm_A(x,y)$ denotes global quality map.

Table 1 (cont). *Quality metrics used for objective evaluation.*

M_7	Nonlinear correlation information entropy [28]	$H^r(X) = -\sum_{i=1}^{b} \frac{n_{ij}}{N} log_b\left(\frac{n_{ij}}{N}\right)$ $M_7(X,Y) = H^r(X) + H^r(Y) - H^r(X,Y)$
M_9	Sum of the correlations of differences [29]	$M_9(F) = c(D_A, F) + c(D_B, F)$

III. EXPERIMENTAL RESULTS

In this section, an objective quality assessment for digital image watermarking using SCO is presented based on various quality metrics. The experiments were conducted on a system running Windows 7, equipped with an i5 2.3 GHz processor, 16 GB RAM, and utilizing Matlab software. The watermarking process was performed using the watermark image depicted in Figure 2 on images commonly employed in image processing, as shown in Figure 2. The resultant numerical outcomes are provided in a comparative analysis with GA, DE, and ABC optimization algorithms. To ensure a fair evaluation, common parameter values were uniformly selected. For the unique parameters of each optimization algorithm, recommended values were employed. The parameter values used for the optimization algorithms are detailed in Table 2. The first column of the table lists the optimization algorithm, followed by the parameter values used in the experiments. Preliminary trials established the maximum number of iterations as 500 for each algorithm, with a population size of 10 for all algorithms except SCO. Due to the probabilistic nature of the optimization algorithms, each was executed independently thirty times. The maximum, mean, and corresponding standard deviation values obtained from these executions are presented in the tables.

Table 2. *The parameter values of the optimization algorithms used in the experiments.*

Algorithms	**Parameter Values**
SCO	m=5, alpha=1000, b=2.4
GA	pc=0.7 mu=0.1
DE	beta_min=0.2, beta_max=0.8, pCR=0.2
ABC	nOnlooker=nPop, L=round(.6*nVar*nPop), a=1

Figure 2. *The image set utilized for the experiments.*

Tables 3-7 present the numerical results obtained from the experiments conducted for digital image watermarking. The first column of the respective tables denotes the name of the optimization algorithms (Alg.). Following this, the maximum (M), average (A), and standard deviation (S) values obtained for each quality metric are provided. Subsequently, the numerical results obtained for each quality metric are listed sequentially. After each quality metric value, the rank (R) of the algorithm in the corresponding quality metric is specified. The final column furnishes the total ranking values (T_R) to facilitate a more straightforward objective evaluation for the readers. The T_R value is calculated by summing the scores each optimization algorithm achieves in descending order of their rank values across all quality metrics. Namely, an optimization algorithm receives a score of 4 when ranked first in any quality metric and a score of 1 when ranked last. Upon examining the pertinent tables, it is observed that the S values are exceedingly low, approaching zero. This indicates that the method exhibits stability in digital image watermarking.

Table 3. *The numerical results obtained for Experiment Image 1.*

Alg.		M_1		M_2		M_3		M_4		M_5		M_6		M_7		M_8		
		Value	R	Value	R	Value	R	Value	R	Value	R	Value	R	Value	R	Value	R	T_R
SCO	M	1331,260		6,973		4,426		36,486		0,429		0,410		0,817		1,103		
	A	1331,185	1	6,971	3	4,423	4	36,485	1	0,429	1	0,410	1	0,817	4	1,103	1	1
	S	0,064		3E-04		5E-04		0,0009		9E-06		2E-05		6E-06		0,0002		
ABC	M	1331,260		6,971		4,424		36,486		0,429		0,410		0,817		1,103		
	A	1331,148	4	6,971	1	4,424	1	36,485	4	0,429	4	0,410	4	0,817	1	1,103	4	4
	S	0,030		6E-05		1E-04		0,0004		2E-06		3E-06		3E-06		8E-05		
DE	M	1331,260		6,971		4,424		36,486		0,429		0,410		0,817		1,103		
	A	1331,164	2	6,971	4	4,423	3	36,485	2	0,429	2	0,410	2	0,817	3	1,103	2	2
	S	0,049		1E-04		2E-04		0,0007		3E-06		5E-06		5E-06		0,0001		
GA	M	1331,260		6,971		4,424		36,486		0,429		0,410		0,817		1,103		
	A	1331,156	3	6,971	2	4,423	2	36,485	3	0,429	3	0,410	3	0,817	2	1,103	3	3
	S	0,042		8E-05		2E-04		0,0006		2E-06		4E-06		4E-06		0,0001		

Table 3 delineates the numerical results acquired for Experiment Set 1 using optimization algorithms, evaluated across various quality metrics. For Image 1, SCO achieved the optimal outcome in five quality metrics, whereas it registered the worst values in M_3 and M_7. Consequently, it is evident that for Image 1, SCO demonstrated the superior performance, followed sequentially by DE, GA, and ABC.

Table 4. *The numerical results obtained for Experiment Image 2.*

Alg.		M_1		M_2		M_3		M_4		M_5		M_6		M_7		M_8		
		Value	**R**	**Value**	**R**	**Value**	**R**	**Value**	**R**	**Value**	**R**	**Value**	**R**	**Value**	**R**	**Value**	**R**	**T_R**
SCO	**M**	2273,255		7,295		4,348		47,679		0,410		0,344		0,822		1,208		
	A	2273,255	1	7,295	1	4,348	3	47,679	1	0,410	1	0,344	1	0,822	1	1,208	1	1
	S	0,000		4E-15		2E-15		2E-14		2E-16		1E-16		3E-16		5E-16		
ABC	**M**	2273,255		7,295		4,351		47,679		0,410		0,344		0,822		1,208		
	A	2272,436	4	7,294	4	4,349	1	47,670	4	0,410	3	0,344	4	0,822	4	1,208	3	4
	S	1,058		8E-04		0,001		0,0111		2E-05		9E-05		8E-05		0,0001		
DE	**M**	2273,255		7,295		4,348		47,679		0,410		0,344		0,822		1,208		
	A	2273,255	1	7,295	1	4,348	3	47,679	1	0,410	1	0,344	1	0,822	1	1,208	1	1
	S	0,000		4E-15		2E-15		2E-14		2E-16		1E-16		3E-16		5E-16		
GA	**M**	2273,255		7,295		4,355		47,679		0,410		0,344		0,822		1,208		
	A	2273,005	3	7,295	3	4,348	2	47,676	3	0,410	4	0,344	3	0,822	3	1,208	4	3
	S	0,696		3E-04		0,001		0,0073		4E-05		0,0002		9E-05		0,0007		

Table 4 delineates the numerical outcomes obtained for Experiment Set 2 using optimization algorithms, assessed based on various quality metrics. For Image 2, SCO exhibited the preeminent performance across all quality metrics except M_3, wherein DE matched SCO's performance. Consequently, for Image 2, it can be inferred that SCO and DE demonstrated equivalent performance, followed by GA and ABC exhibiting relatively superior performance in that order.

Table 5. *The numerical results obtained for Experiment Image 3.*

Alg.		M_1		M_2		M_3		M_4		M_5		M_6		M_7		M_8		
		Value	**R**	**Value**	**R**	**Value**	**R**	**Value**	**R**	**Value**	**R**	**Value**	**R**	**Value**	**R**	**Value**	**R**	**T_R**
SCO	**M**	2978,976		7,619		4,410		54,580		0,415		0,438		0,818		1,378		
	A	2978,183	3	7,619	2	4,409	3	54,573	3	0,415	3	0,438	2	0,818	4	1,378	3	3
	S	0,348		2E-04		3E-04		0,0032		2E-05		4E-05		6E-06		4E-05		
ABC	**M**	2981,680		7,620		4,417		54,605		0,416		0,438		0,818		1,378		
	A	2979,453	1	7,619	4	4,410	1	54,584	1	0,416	1	0,438	4	0,818	1	1,378	1	1
	S	1,170		5E-04		0,002		0,0107		0,0003		0,0001		3E-05		0,0002		
DE	**M**	2978,976		7,619		4,410		54,580		0,415		0,438		0,818		1,378		
	A	2978,111	4	7,619	1	4,409	4	54,572	4	0,415	4	0,438	1	0,818	3	1,378	4	4
	S	0,345		2E-04		3E-04		0,0032		5E-06		1E-05		8E-06		4E-05		
GA	**M**	2981,302		7,619		4,417		54,601		0,416		0,438		0,818		1,378		
	A	2978,611	2	7,619	3	4,410	2	54,577	2	0,415	2	0,438	3	0,818	2	1,378	2	2
	S	0,959		3E-04		0,002		0,0088		0,0002		8E-05		2E-05		0,0001		

Table 5 presents the numerical results obtained for Experiment Set 3 using optimization algorithms, assessed across various quality metrics. For Image 3, the ABC algorithm exhibited superior performance across all quality metrics except M2 and M6. Therefore, for digital image watermarking of Image 3, the

ranking of performance is as follows: ABC, GA, SCO, and DE. It can be inferred that SCO did not demonstrate commendable performance for this image.

Table 6. *The numerical results obtained for Experiment Image 4.*

Alg.		M_1		M_2		M_3		M_4		M_5		M_6		M_7		M_8		
		Value	R	Value	R	Value	R	Value	R	Value	R	Value	R	Value	R	Value	R	T_R
SCO	M	2343,499		7,534		6,987		48,410		0,494		0,437		0,817		1,319		
	A	2343,012	3	7,534	3	6,986	4	48,405	3	0,494	3	0,437	1	0,817	2	1,319	2	2
	S	0,775		2E-04		2E-04		0,008		1E-05		4E-05		9E-06		0,0002		
ABC	M	2351,873		7,542		6,990		48,496		0,494		0,437		0,817		1,320		
	A	2343,025	2	7,535	1	6,987	1	48,405	2	0,494	4	0,437	4	0,817	4	1,319	4	3
	S	1,916		0,001		0,001		0,0198		0,0001		0,0002		8E-05		0,0003		
DE	M	2343,499		7,534		6,987		48,410		0,494		0,437		0,817		1,319		
	A	2343,434	1	7,534	4	6,987	2	48,409	1	0,494	2	0,437	3	0,817	1	1,319	1	1
	S	0,196		2E-04		4E-05		0,002		5E-08		1E-06		2E-06		6E-05		
GA	M	2343,499		7,535		6,989		48,410		0,494		0,437		0,817		1,319		
	A	2342,985	4	7,534	2	6,987	3	48,404	4	0,494	1	0,437	2	0,817	3	1,319	3	3
	S	0,704		3E-04		5E-04		0,0073		2E-05		8E-05		1E-05		0,0002		

Table 6 delineates the numerical results obtained for Experiment Set 4 utilizing optimization algorithms, evaluated based on various quality metrics. For Image 4, it can be posited that DE demonstrated superior performance relative to the others, while GA and ABC exhibited equally performance, trailing SCO.

Table 7. *The numerical results obtained for Experiment Image 5.*

Alg.		M_1		M_2		M_3		M_4		M_5		M_6		M_7		M_8		
		Value	R	Value	R	Value	R	Value	R	Value	R	Value	R	Value	R	Value	R	T_R
SCO	M	2607,305		7,440		4,655		51,062		0,434		0,388		0,819		1,152		
	A	2607,231	2	7,440	1	4,655	1	51,061	2	0,434	1	0,388	4	0,819	2	1,152	1	1
	S	0,053		3E-05		2E-04		0,0005		6E-06		2E-05		2E-06		2E-05		
ABC	M	2607,305		7,440		4,655		51,062		0,434		0,388		0,819		1,152		
	A	2606,953	3	7,440	2	4,655	3	51,058	3	0,434	3	0,388	2	0,819	3	1,152	2	3
	S	0,600		6E-04		9E-04		0,0059		3E-05		0,0001		1E-05		0,0003		
DE	M	2611,984		7,440		4,655		51,108		0,434		0,388		0,819		1,152		
	A	2607,276	1	7,440	3	4,655	2	51,061	1	0,434	4	0,388	3	0,819	1	1,152	3	2
	S	1,010		9E-04		0,002		0,0099		0,0002		0,0001		2E-05		0,0004		
GA	M	2607,305		7,440		4,655		51,062		0,434		0,388		0,819		1,152		
	A	2606,800	4	7,440	4	4,654	4	51,057	4	0,434	2	0,388	1	0,819	4	1,151	4	4
	S	0,667		7E-04		0,001		0,0065		2E-05		0,0002		1E-05		0,0004		

Table 7 provides the numerical results obtained for Experiment Set 5 using optimization algorithms, evaluated across various quality metrics. For Image 5, it can be asserted that SCO demonstrated the best performance in four quality metrics and the second-best performance in three other metrics. Conversely, it is evident that GA exhibited the poorest performance. Thus, for digital watermarking of Image 5, the algorithms' performance can be ranked in the following order: SCO, DE, ABC, and GA.

In Table 8, the computational cost of the optimization algorithms is delineated. The table's initial column enumerates the algorithms subjected to comparison, followed by the stamping time for each individual image. Upon scrutinizing the table, it can be discerned that the SCO algorithm demonstrates a markedly superior computational speed relative to its counterparts. It is further observable that DE succeeds SCO, trailed by ABC, and ultimately by GA, in terms of computational duration. Thus, it may be posited that, for digital image watermarking, SCO exhibits a computational efficiency that surpasses the other algorithms included in the comparison.

Table 8. *Comparative evaluation of algorithmic computation times*

	Image Set				
	1	**2**	**3**	**4**	**5**
SCO	0.843273	0.832979	0.822952	0.827584	0.813185
GA	2.956.302	2.184.961	2.286.389	2.267.131	2.232.963
DE	2.042.678	1.942.010	1.972.971	1.924.230	1.955.935
ABC	2.197.032	2.155.925	2.181.180	2.242.619	2.240.701

In the evaluation of watermarked images, a single quality metric proves inadequate, and solely relying on objective assessment also falls short. Alongside objective evaluation, subjective assessment is essential. Figure 3 illustrates the watermarked images obtained from the conducted experiments. Due to the proximity of the numerical results and the similarity among the watermarked images, there is no discernible visual difference, which precludes the possibility of conducting a subjective evaluation.

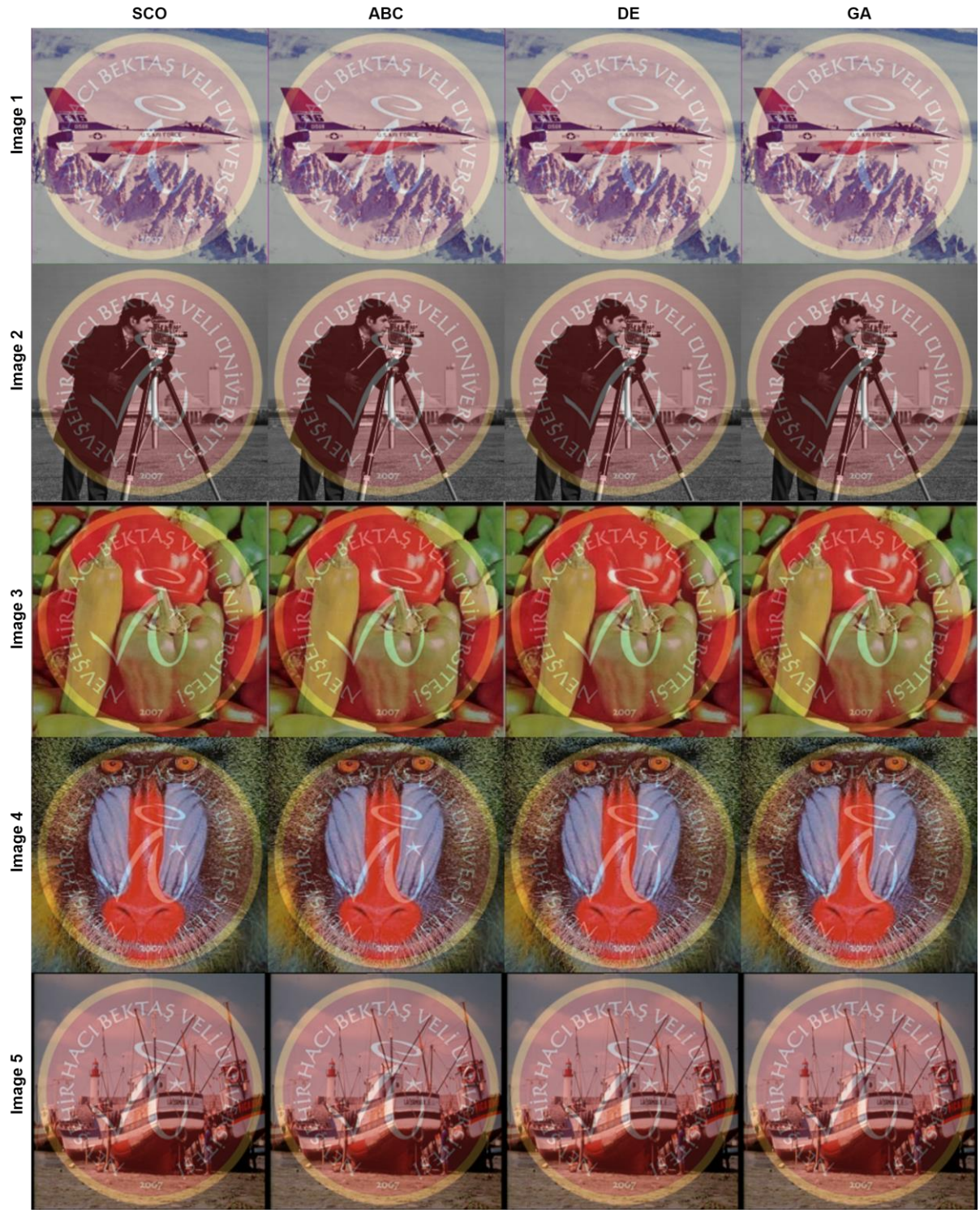

Figure 3. *The obtained watermarked images*

As illustrated in Figure 3, although the numerical results of the optimization algorithms vary across all image sets, there is no discernible visual distinction among the resulting watermarked images. Thus, it can be inferred that the optimization algorithms employed in this study yield comparable results in terms of subjective evaluation for visible digital watermarking.

IV. CONCLUSION

In summation, the advent of digital image watermarking, particularly through the employment of the Single Candidate Optimizer (SCO), proffers a significant advancement in the realm of copyright protection amidst the burgeoning ease of information accessibility afforded by internet technologies. This study elucidates the efficacy of SCO, a non-population-based algorithm, in optimizing the congruence between watermarked images and their respective host and watermark counterparts. Numerical evaluations, conducted on standard image processing datasets and assessed via an octet of quality metrics, substantiate the superiority of SCO over traditional metaheuristic algorithms such as genetic algorithm, differential evolution, and artificial bee colony optimization. The preeminence of SCO is further accentuated by its expeditious performance, attributable to its non-population-based framework. Consequently, SCO emerges as a paramount technique for visible digital image watermarking, offering enhanced fidelity and computational efficiency.

In this study, the host image is considered in its entirety, and an optimal fusion coefficient is accordingly derived. Given that natural images do not encompass homogeneous information, the uniform application of the derived fusion coefficient across the entire image may engender undesirable artifacts in the watermarked image. To obviate this issue, methodologies could be devised whereby the host image is partitioned into blocks, with distinct fusion coefficients ascertained for each block. Furthermore, methods that optimize the commonly employed block size in image fusion could be implemented to evaluate the results.

ACKNOWLEDGEMENTS: The author declares no conflict of interest.
AUTHOR CONTRIBUTIONS (COMPULSORY): This article is submitted by a single author.

V. REFERENCES

[1] H. Akbulut, V. Aslantas, and H. Ulutaş, "Visible Image Watermarking Based on Image Fusion with Shearlet Transform Using Genetic Algorithm," *Electronic Letters on Science and Engineering*, vol. 13, no. 3, pp. 1-9, 2017.

[2] Singh, R. et al. "From classical to soft computing based watermarking techniques: A comprehensive review", *Future Generation Computer Systems*, vol. 141, pp. 738–754, 2023.

[3] A. Anand and A. K. Singh, "Dual Watermarking for Security of COVID-19 Patient Record," *IEEE Transactions on Dependable and Secure Computing*, vol. 20, no. 1, pp. 859–866, Jan. 2023

[4] S. Roy and A. K. Pal, "An indirect watermark hiding in discrete cosine transform–singular value decomposition domain for copyright protection," *Royal Society Open Science*, vol. 4, no. 6, p. 170326, Jun. 2017

[5] A. K. Abdulrahman and S. Ozturk, "A novel hybrid DCT and DWT based robust watermarking algorithm for color images," *Multimedia Tools and Applications*, vol. 78, no. 12, pp. 17027–17049, Jan. 2019

[6] S. M. Darwish and L. D. S. Al-Khafaji, "Dual Watermarking for Color Images: A New Image Copyright Protection Model based on the Fusion of Successive and Segmented Watermarking," *Multimedia Tools and Applications*, vol. 79, no. 9–10, pp. 6503–6530, Dec. 2019

[7] H. Mittal and M. Saraswat, "An optimum multi-level image thresholding segmentation using non-local means 2D histogram and exponential Kbest gravitational search algorithm," *Engineering Applications of Artificial Intelligence*, vol. 71, pp. 226–235, May 2018

[8] Y. Wang, Y. Yu, S. Gao, H. Pan, and G. Yang, “A hierarchical gravitational search algorithm with an effective gravitational constant,” *Swarm and evolutionary computation*, vol. 46, pp. 118–139, May 2019

[9] P. Rawal, H. Sharma, and N. Sharma, “Fast Convergent Gravitational Search Algorithm,” in *Algorithms for intelligent systems*, 2020, pp. 1–12

[10] H. Mittal and M. Saraswat, “An automatic nuclei segmentation method using intelligent gravitational search algorithm based superpixel clustering,” *Swarm and Evolutionary Computation*, vol. 45, pp. 15–32, Mar. 2019

[11] V. Aslantas, S. Ozer and S. Ozturk, "A novel image watermarking method based on Discrete Cosine Transform using Genetic Algorithm," *2009 IEEE 17th Signal Processing and Communications Applications Conference*, Antalya, Turkey, 2009, pp. 285-288

[12] C. Zhang and M. Hu, "Curvelet Image Watermarking Using Genetic Algorithms," *2008 Congress on Image and Signal Processing*, Sanya, China, 2008, pp. 486-490

[13] B. Jagadeesh, S. S. Kumar and K. R. Rajeswari, "Image Watermarking Scheme Using Singular Value Decomposition, Quantization and Genetic Algorithm," *2010 International Conference on Signal Acquisition and Processing*, Bangalore, India, 2010, pp. 120-124

[14] R. Çolak, T. Yiğit, “Üniversite Ders Çizelgeleme Probleminin Genetik Algoritma ile Optimizasyonu”, *Düzce Üniversitesi Bilim ve Teknoloji Dergisi*, c. 9, s. 6, ss. 150-166, 2021

[15] T. Timuçin, S. Biroğul, “Hibrit Genetik Algoritma Kullanarak Ameliyat Odası Çizelgeleme”, *Düzce Üniversitesi Bilim ve Teknoloji Dergisi*, c. 10, s. 1, ss. 255-274, 2022

[16] M. N. Demir, Y. Altun, “Otonom Araçla Genetik Algoritma Kullanılarak Haritalama ve Lokasyon”, *Düzce Üniversitesi Bilim ve Teknoloji Dergisi*, c. 8, s. 1, ss. 654-666, 2020

[17] R. Özdemir, M. Taşyürek, and V. Aslantaş, “Improved Marine Predators Algorithm and Extreme Gradient Boosting (XGBoost) for shipment status time prediction,” *Knowledge-Based Systems*, vol. 294, p. 111775, Apr. 2024

[18] T. M. Shami, D. Grace, A. Burr, and P. D. Mitchell, “Single candidate optimizer: a novel optimization algorithm,” *Evolutionary Intelligence*, Aug. 2022

[19] J. H. Holland, Adaptation in natural and artificial systems: an introductory analysis with applications to biology, *control and artificial intelligence*. Ann Arbor, Mich, 1975.

[20] R. Storn and K. Price, “Differential Evolution – A Simple and Efficient Heuristic for global Optimization over Continuous Spaces,” *Journal of Global Optimization*, vol. 11, no. 4, pp. 341–359, Jan. 1997

[21] D. Karaboga and B. Basturk, “A powerful and efficient algorithm for numerical function optimization: artificial bee colony (ABC) algorithm,” *Journal of Global Optimization*, vol. 39, no. 3, pp. 459–471, Apr. 2007

[22] V. Aslantas and R. Kurban, “A comparison of criterion functions for fusion of multi-focus noisy images,” *Optics Communications*, vol. 282, no. 16, pp. 3231–3242, Aug. 2009

[23] K. Ma, Kai Zeng, and Zhou Wang, “Perceptual Quality Assessment for Multi-Exposure Image Fusion,” *IEEE Transactions on Image Processing*, vol. 24, no. 11, pp. 3345–3356, Nov. 2015

[24] A. M. Eskicioglu and P. S. Fisher, “Image quality measures and their performance,” *IEEE Transactions on Communications*, vol. 43, no. 12, pp. 2959–2965, 1995

[25] Y. Liu, S. Liu, and Z. Wang, “A general framework for image fusion based on multi-scale transform and sparse representation,” *Information Fusion*, vol. 24, pp. 147–164, Jul. 2015

[26] C. S. Xydeas and PetrovićV., “Objective image fusion performance measure,” *Electronics Letters*, vol. 36, no. 4, p. 308, 2000

[27] Y. Chen and R. S. Blum, “A new automated quality assessment algorithm for image fusion,” *Image and Vision Computing*, vol. 27, no. 10, pp. 1421–1432, Sep. 2009

[28] H. Wang and X. Yao, “Objective reduction based on nonlinear correlation information entropy,” *Soft Computing*, vol. 20, no. 6, pp. 2393–2407, Mar. 2015

[29] V. Aslantas and E. Bendes, “A new image quality metric for image fusion: The sum of the correlations of differences,” *AEU - International Journal of Electronics and Communications*, vol. 69, no. 12, pp. 1890–1896, Dec. 2015